Inorg. Chem. **2004**, *43*, 8236–8238

Inorganic Chemistry
Communication

Theoretical Study of the Gas-Phase $Fe(CO)_5$ Catalyzed Water Gas Shift Reaction: A New Mechanism Proposed

Susan E. Barrows*

Penn State Capital College, School of Science Engineering and Technology, 200 University Drive, Schuylkill Haven, Pennsylvania 17972

Received June 28, 2004

A novel mechanism for the gas-phase $Fe(CO)_5$ and base catalyzed water gas shift reaction has been examined. The reaction pathway described here is predicted at the B3LYP/6-31++G(d,p) level to be energetically competitive with the classic mechanism. The reaction path explored here involves the energetically barrierless formation of $(CO)_4FeCOOH^-$ (the catalyst of the system) decarboxylation induced by the addition of CO to give $(CO)_4FeCHO$, and evolution of H_2 upon addition of H_2O to the $(CO)_4FeCHO$ intermediate. The energetic barriers predicted for the last two steps are 21.2 and 42.0 kcal/mol, respectively, using the B3LYP method.

The water gas shift reaction (WGSR) (reaction 1) is an important side reaction of CO that enriches the H_2 concentration of syngas (CO and H_2 mixture) in fuel cells and in the Fischer−Tropsch (F−T) process.

$$CO(g) + H_2O(g) \rightarrow H_2(g) + CO_2(g) \qquad (1)$$

As early as 1930, homogeneous catalysis of the WGSR by transition metal carbonyls was known to allow the reaction to occur at temperatures significantly lower than those used in fuel cells and (F−T) converters. After much investigation, a mechanism for the $Fe(CO)_5$ catalyzed WGSR cycle was formulated involving a series of experimentally substantiated individual reactions.[1,2] The individual steps of the catalytic cycle were examined in the gas phase by Sunderlin and Squires, and a reaction profile for the cycle was derived.[3] This mechanism was critically examined in a theoretical study conducted by Torrent and co-workers.[4] As a result of their work, a slightly more detailed mechanism was proposed (Scheme 1). Their thermodynamic results are listed in Table 1. The minima and transition state structures for the first five steps proposed by Torrent were recalculated here using the standard 6-31++G(d,p) basis set in Gaussian 03.[5] The results are presented in Table 1.

Scheme 1. Mechanism Proposed by Torrent and Co-Workers for $Fe(CO)_5$ Catalyzed WGSR

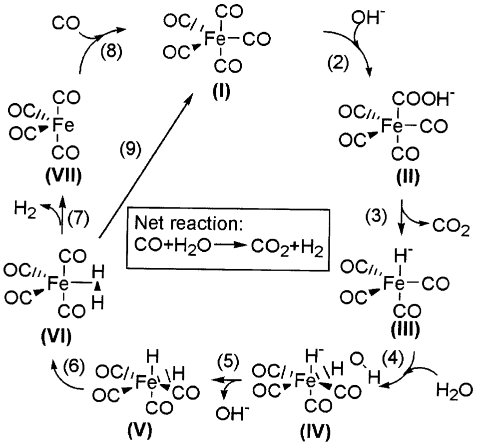

Scheme 2. Newly Proposed Mechanism for $Fe(CO)_5$ Catalyzed WGSR

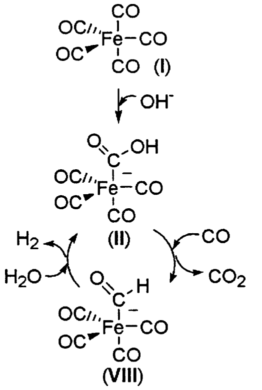

Arguments against this classically proposed mechanism center on reactions 7 and 8.[6] Experimental evidence suggests that CO should be involved in the elimination of H_2 from **VI**. Rate studies of the ruthenium-based catalyzed WGSR in alkaline solution indicate a first-order rate dependence on P_{CO}.[7] Since in this mechanism CO adds to a coordinatively unsaturated $Fe(CO)_4$, this could not be the rate determining step of the process.

---

* E-mail: seb16@psu.edu.

[1] Brice, N.; Kao, S. C.; Pettit, R. *J. Am. Chem. Soc.* **1979**, *101*, 1627.

[2] Lane, K. R.; Lee, R. E.; Sallans, L.; Squires, R. R. *J. Am. Chem. Soc.* **1984**, *106*, 5767.

[3] Sunderlin, L. S.; Squires, R. R. *J. Am. Chem. Soc.* **1993**, *115*, 337

[4] Torrent, M.; Sola, M.; Frenking, G. *Organometallics* **1999**, *18*, 2801.

10.1021/ic049159t CCC: $27.50

Table 1. B3LYP/6-31++G(d,p) Calculated Energies ΔE (kcal/mol) for Reactions Illustrated in Scheme 1

reaction number	reaction	ΔE B3LYP/6-31++G(d,p)[6] (previous)	ΔE B3LYP/6-31++G(d,p) (current)
2	$Fe(CO)_5$ (**I**) + OH^- → $(CO)_4FeCOOH^-$ (**II**)	−70.5 (−65.8)[a]	−71.8 (−67.6)[a]
3	$(CO)_4FeCOOH^-$ (**II**) → $(CO)_4FeH^-$ (**III**) + CO_2	−3.9 (−7.3)	−1.6 (−5.0)
4	$(CO)_4FeH^-$ (**III**) + H_2O → $(CO)_4FeH^{\bullet -}H_2O$ (**IV**)	−7.0 (−3.4)	−7.5 (−5.9)
5	$(CO)_4FeH^{\bullet -}H_2O$ (**IV**) → $(CO)_4FeH_2$ (**V**) + OH^-	82.6 (78.5)	84.3 (80.5)
6	$(CO)_4FeH_2$ (**V**) → $(CO)_4FeH_2$ (**VI**)	7.9 (7.7)	6.4 (6.6)
7	$(CO)_4FeH_2$ (**VI**) → $Fe(CO)_4$ (**VII**) + H_2	17.5 (13.2)	
8	$Fe(CO)_4$ (**VII**) + CO → $Fe(CO)_5$ (**I**)	−37.9 (−35.1)	
9	$(CO)_4FeH_2$ (**VI**) + CO → $Fe(CO)_5$ (**I**) + H_2		−21.1 (−22.8)
1	CO + H_2O → H_2 + CO_2	−11.3 (−14.1)	−11.3 (−14.2)

	transition state structure	$\Delta E^\ddagger$ B3LYP/6-31++G(d,p)[3]	$\Delta E^\ddagger$ B3LYP/6-31++G(d,p)
3	TS (**II−III**)	33.1 (29.4)	33.8 (29.5)
9	TS (**VI−I**)		17.4 (29.3)

[a] Numbers in parentheses include ZPE corrections.

An S_N2-like reaction in which CO replaces H_2 in **VI** (reaction 9, Scheme 1) was explored by Torrent, who approximated that transition state structure lies 28.9 kcal/mol above separated reactants. He thus concluded that "the reaction should proceed through the less-demanding path despite not being fully consistent with the experimental facts."[4] In this work, we were able to locate such a transition state structure. The incoming CO was found to approach from the same side as the H_2 ligand (approximately 63° angle to the leaving H_2). The B3LYP/6-31++G(d,p) optimized geometry (TS (**VI−I**) reaction 9) is illustrated in Figure 1. The transition state lies 29.3 kcal/mol higher in energy than reactants and represents the highest energy structure on the reaction profile. With this transition state structure located, we can verify Torrent's conclusion that this mechanism is not completely consistent with all known experimental facts. The thermodynamic profile for the catalytic cycle involving reactions 2−8 as calculated by Torrent and co-workers is illustrated in Figure 2. Also shown in Figure 2 is the agreement between the results of his work and the current work.

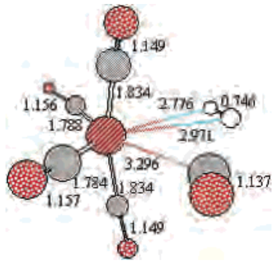

Figure 1. B3LYP/6-31++G(d,p) optimized TS (**VI−I**). This structure corresponds to CO substitution of H_2 and thus would account for the observed first-order rate dependence on CO. However, the current calculations and work by Torrent do not support this mechanism.

The base and $Fe(CO)_5$ mediated WGSR was explored further in order to determine if theory predicts the existence of an alternative mechanism. In addition to the problems discussed above with reactions 7 and 8, our concern was with the energetic cost of the slowest step in the mechanism, reaction 5.[8−10] The energy barrier to this step is approximately 80 kcal/mol. In the classical mechanism, the highest energy intermediate is calculated to be 20.9 kcal/mol higher than the starting materials.

In the course of this investigation, a new and more direct mechanism was discovered. The new mechanism proceeds through the following three steps process:

$$Fe(CO)_5\,(\mathbf{I}) + OH^- \rightarrow (CO)_4FeCOOH^-\,(\mathbf{II}) \tag{2}$$

$$(CO)_4FeCOOH^-\,(\mathbf{II}) + CO \rightarrow (CO)_4FeCHO^-\,(\mathbf{VIII}) + CO_2 \tag{10}$$

$$(CO)_4FeCHO^-\,(\mathbf{VIII}) + H_2O \rightarrow (CO)_4FeCOOH^-\,(\mathbf{II}) + H_2 \tag{11}$$

It has been reported that the activation of the $Fe(CO)_5$ catalysis by OH^- to produce **II** is a barrierless and highly exothermic process.[3,4] Thus, it was assumed that reaction 2 is the first reaction of the mechanism. Addition of CO to **II** (reaction 10) results in the elimination of CO_2 from the carboxylate ligand and concomitant migration of hydrogen to the incoming CO to produce the formyl group. Similar to the H_2 substitution by CO step discussed previously, CO approaches the leaving CO_2 ligand at a 59.3° angle in the transition state (see TS (**II−VIII**), Figure 4). Thermodynamic data for reactions 2, 10, and 11 are listed in Table 2. The energetic barrier to this reaction is 21.2 kcal/mol including ZPE correction. This value is 8.3 kcal/mol lower in energy than TS (**II−III**) in reaction 3.

TS (**II−VIII**) involves a less strained five-membered ring structure in comparison to the four-membered ring structure in TS (**II−III**). Once **III** is formed in the mechanism

---

(5) Frisch, M. J.; Trucks, G. W.; Schlegel, H. B.; Scuseria, G. E.; Robb, M. A.; Cheeseman, J. R.; Montgomery, J. A., Jr.; Vreven, T.; Kudin, K. N.; Burant, J. C.; Millam, J. M.; Iyengar, S. S.; Tomasi, J.; Barone, V.; Mennucci, B.; Cossi, M.; Scalmani, G.; Rega, N.; Petersson, G. A.; Nakatsuji, H.; Hada, M.; Ehara, M.; Toyota, K.; Fukuda, R.; Hasegawa, J.; Ishida, M.; Nakajima, T.; Honda, Y.; Kitao, O.; Nakai, H.; Klene, M.; Li, X.; Knox, J. E.; Hratchian, H. P.; Cross, J. B.; Adamo, C.; Jaramillo, J.; Gomperts, R.; Stratmann, R. E.; Yazyev, O.; Austin, A. J.; Cammi, R.; Pomelli, C.; Ochterski, J. W.; Ayala, P. Y.; Morokuma, K.; Voth, G. A.; Salvador, P.; Dannenberg, J. J.; Zakrzewski, V. G.; Dapprich, S.; Daniels, A. D.; Strain, M. C.; Farkas, O.; Malick, D. K.; Rabuck, A. D.; Raghavachari, K.; Foresman, J. B.; Ortiz, J. V.; Cui, Q.; Baboul, A. G.; Clifford, S.; Cioslowski, J.; Stefanov, B. B.; Liu, G.; Liashenko, A.; Piskorz, P.; Komaromi, I.; Martin, R. L.; Fox, D. J.; Keith, T.; Al-Laham, M. A.; Peng, C. Y.; Nanayakkara, A.; Challacombe, M.; Gill, P. M. W.; Johnson, B.; Chen, W.; Wong, M. W.; Gonzalez, C.; Pople, J. A. *Gaussian 03*, revision A.1; Gaussian, Inc.: Pittsburgh, PA, 2003.

(6) Torrent, M.; Sola, M.; Frenking, G. *Chem. Rev.* **2000**, *100*, 439 (and references therein).

(7) Ford, P. C.; Rinker, R. G.; Ungermann, C.; Laine, R. M.; Landis, V.; Moya, S. A. *J. Am. Chem. Soc.* **1978**, *100*, 4595.

(8) Kang, H.; Mauldin, C.; Cole, T.; Slegeir, W.; Petit, R. *J. Am. Chem. Soc.* **1977**, *99*, 8323.

(9) Gross, D. C.; Ford, P. C. *Inorg. Chem.* **1982**, *21*, 1704.

(10) Amovilli, C.; Floris, F. M.; Sola, M.; Tomasi, J. *Organometallics* **2001**, *20*, 1310.

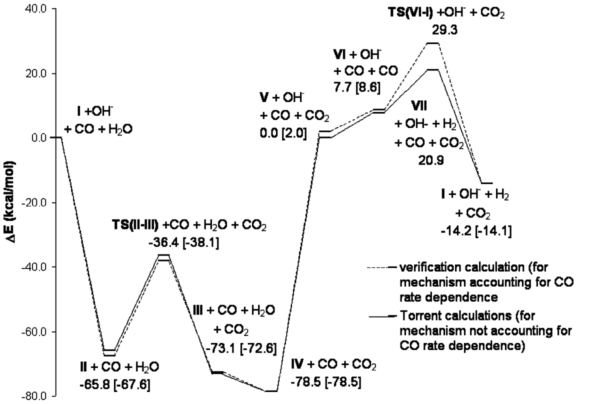

Figure 2. Reaction profile for $Fe(CO)_5$ catalyzed WGSR. The solid line connects values calculated at the B3LYP/6-31++G(d,p) level with ZPE correction. The dashed line connects values, in brackets, calculated for verification of the methods used in this paper.

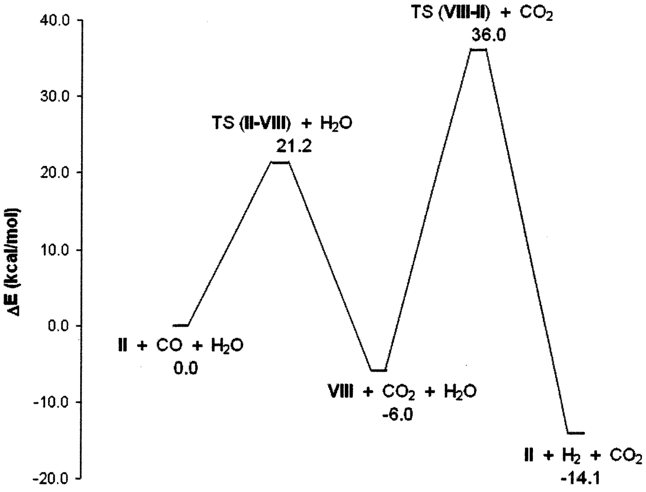

Figure 3. Reaction profile for $Fe(CO)_5$ catalyzed WGSR calculated at B3LYP/6-31++G(d,p) level with ZPE correction.

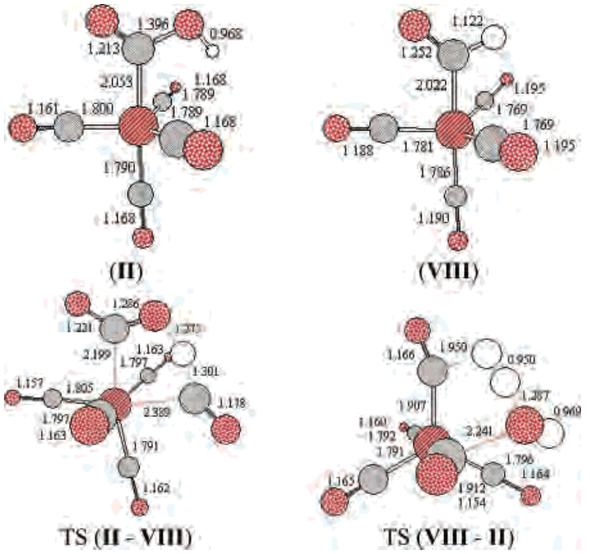

Figure 4. B3LYP/6-31++G(d,p) optimized minima and transition states structures involved in the newly proposed $Fe(CO)_5$ catalyzed WGSR mechanism.

Table 2. Calculated Reaction Energies Δ*E* (kcal/mol) for Steps 2, 10, and 11

reaction number	Δ*E* B3LYP/6-31++G(d,p)
2	−71.8 (−67.6)
10	−6.6 (−6.0)
11	−4.6 (−8.2)

transition state structures	$\Delta E^{\ddagger}$ B3LYP/6-31++G(d,p)
10 TS (**II**−**VIII**)	22.8 (21.2)
11 TS (**VIII**−**II**)	46.7 (42.0)

illustrated in Scheme 1, it is predicted to complex with water, forming **IV**. Intermediate **IV** is favored thermodynamically over **VIII** by 2.9 kcal/mol; thus, its formation would constitute a competitive reaction path to the proposed mechanism.

The next step, reaction 11, involves a dissociative addition of water to **VIII** and elimination of H_2. This step of the process is calculated to have a reaction barrier of 42.0 kcal/mol with ZPE included. With **II** being reformed at this step in the process, the catalytic cycle is complete without the need to reform **I**.

The highest point, energetically, on the reaction pathway of the catalytic cycle in the classic mechanism (Scheme 1) is 20.9 kcal/mol above the starting materials. However, in order for the classic mechanism to proceed past **IV**, three consecutive endothermic steps, totaling 99.4 kcal/mol of energy, must occur. The slowest step in the process has a calculated activation energy of 78.5 kcal/mol. The highest point on the reaction pathway, TS (**VIII**−**II**), for the catalytic cycle proposed here is 36.0 kcal/mol above the energy of **II** (Figure 3). The calculated activation energy for the slowest step is 42.0 kcal/mol. In comparison to the classic mechanism, this transition state structure lies 31.6 kcal/mol below the starting materials.

The density function method B3LYP[11] as implemented in Gaussian 03[5] was used in this study. Geometry optimization calculations were performed using the standard 6-31++G(d,p) basis. Vibrational frequencies were calculated at the B3LYP/6-31++G(d,p) level for the characterization of all stationary points and transition state structures and the calculation of zero point energy corrections.

Theory predicts that the mechanism presented (Scheme 2) is an energetically feasible pathway. Importantly, this mechanism explains the first-order rate dependence on CO. Future work includes the theoretical examination of the WGSR with ruthenium-based catalysis for a similar reaction pathway.

Note Added after ASAP Publication: The graphic in Scheme 2 was incorrect in the version of this paper published on the Web on December 1, 2004. The version published on the Web December 7, 2004, has been corrected.

IC049159T

---

(11) Becke, A. D. *J. Chem. Phys.* **1993**, *98*, 5648. Lee, C.; Yang, W.; Parr, R. G. *Phys. Rev.* **1988**, *B37*, 785.